# Broadband 100-W *Ka*-Band SSPA Based on GaN Power Amplifiers

Philipp Neininger, L. John, M. Zink, D. Meder, M. Kuri, A. Tessmann, C. Friesicke, *Member, IEEE*, M. Mikulla, R. Quay, *Senior Member, IEEE*, and Thomas Zwick, *Fellow, IEEE*

***Abstract*— In this letter, we report on the realization of a two-stage 16-way solid-state power amplifier (SSPA) in the *Ka*-band. To this end, we describe the design of a high-power amplifier (HPA) in a 100-nm gallium nitride (GaN) process and its integration into a split-block waveguide module. The PA module achieves an output power of more than 7.6 W between 28 and 39 GHz. In conjunction with 16 of these PA modules, we then employed a custom low-loss radial splitter and combiner to create a compact SSPA system. The two-stage SSPA configuration exhibits a small-signal gain of up to 44 dB and a peak output power of 127 W at 31 GHz in 5 dB of gain compression. Furthermore, we measured output power of close to 100 W and state-of-the-art efficiency values of more than 19% between 28 and 38 GHz. To our knowledge, this is the most broadband high-power SSPA demonstrated so far in this frequency range.**

***Index Terms*— Gallium nitride, *Ka*-band, power combining, solid-state power amplifier (SSPA), waveguide.**

## I. Introduction

With the introduction of the fifth-generation mobile communication and in future communication standards, the required data rates are steadily on the rise. To enable the transmission of these data volumes, the adoption of significantly higher operating frequencies is crucial. In this context, the millimeter-wave (mmW) spectrum between 30 and 300 GHz is arguably the most promising candidate. Using higher frequencies, larger absolute bandwidths can be allocated, allowing for significantly higher data rates. On the other hand, the free-space attenuation is considerably increased. As a result, relatively high output powers in the order of 100 W and more are needed for some future systems.

In recent years, as solid-state transistor technologies continue to improve performance at mmW frequencies, they have evolved to be a tangible alternative in applications that could previously only be realized using traveling-wave tube amplifiers (TWTAs). However, the output power delivered by power amplifiers (PAs) realized using a single microwave monolithic integrated circuit (MMIC) is still severely limited. PA MMICs based on gallium nitride (GaN) have been shown to deliver the highest power density in the lower mmW region. Due to limitations in efficiency and device cooling, $P_{\text{out}}$ in continuous-wave (CW) mode is limited to around 20 W in the *Ka*-band [1]–[5].

Consequently, to reach an output power in the range of 100 W and more, a large-scale power combining approach is essential. In conjunction with a suitable power splitter and combiner, a number of unit amplifiers form a solid-state PA (SSPA). In the *W*-band, the state-of-the-art is set by Schellenberg *et al.* [6], who reported on a full-band SSPA with an average output power of 37 W. In the lower end of the mm-wave spectrum, Yoon *et al.* [7] showed a saturated $P_{\text{out}}$ of greater than 100 W between 27 and 31 GHz. Furthermore, a recent product by Qorvo Inc. provides a $P_{\text{out}}$ of over 105 W between 32 and 38 GHz [8].

It can be seen that the state-of-the-art in *Ka*-band SSPAs is limited in its relative bandwidth to below 18%. However, for multiband communication terminals and high-power measurement equipment, significantly larger bandwidths would be highly beneficial. Consequently, in this letter, we describe the development and evaluation of a compact broadband and high-power SSPA covering most of the *Ka*-band.

## II. Technology

The MMIC process used for this project is required to provide both a large bandwidth and high output power density. Therefore, a GaN-on-SiC technology with a nominal drain voltage of 15 V was used. It features 100-nm T gates, a complete frontside process with two metal layers, air bridges, nickel–chromium resistors, and MIM capacitors. Moreover, through-substrate vias and backside metalization are available. The silicon carbide substrate thickness amounts to 75 $\mu$m.

For increased reliability, a final passivation layer was applied to all MMICs presented in this publication. Typically, this process delivers a power density of 2 W/mm and enables designs at *W*-band and beyond [9].

## III. HPA-Module Design and Measurements

A micrograph of the developed high-power amplifier (HPA) MMIC is depicted in Fig. 1. It features three stages

Manuscript received February 17, 2022; revised March 29, 2022; accepted April 3, 2022. Date of publication April 27, 2022; date of current version June 7, 2022. This work was supported in part by the Federal Office of Bundeswehr Equipment, Information Technology and In-Service Support (BAAINBw) through the Project Subsys and in part by the Research Fab Microelectronics Germany (FMD) funded by the Federal Ministry of Education and Research (BMBF). *(Corresponding author: Philipp Neininger.)*

Philipp Neininger, L. John, M. Zink, D. Meder, M. Kuri, A. Tessmann, C. Friesicke, M. Mikulla, and R. Quay are with the Fraunhofer Institute for Applied Solid State Physics (IAF) 79108 Freiburg im Breisgau, Germany (e-mail: philipp.neininger@iaf.fraunhofer.de).

Thomas Zwick is with the Institute of Radio Frequency Engineering and Electronics (IHE), Karlsruhe Institute of Technology (KIT), 76131 Karlsruhe, Germany.

This article was presented at the IEEE MTT-S International Microwave Symposium (IMS 2022), Denver, CO, USA, June 19–24, 2022.

Color versions of one or more figures in this letter are available at https://doi.org/10.1109/LMWC.2022.3166563.

Digital Object Identifier 10.1109/LMWC.2022.3166563

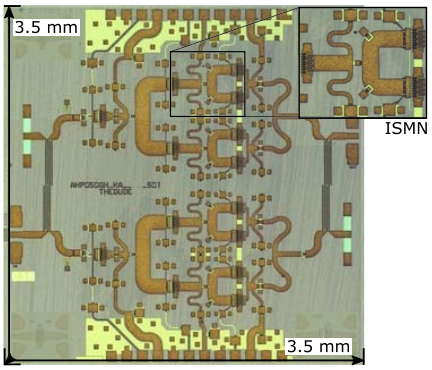


Fig. 1. Micrograph of the developed three-stage high-PA MMIC.

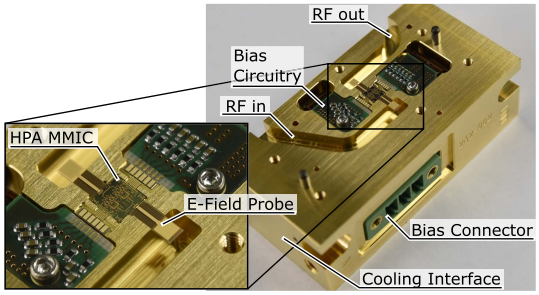


Fig. 2. Split-block amplifier module manufactured for this work. It contains the HPA MMIC, transitions to the WR-28 waveguide, and biasing circuitry.

with a staging ratio of 1:2 each, which results in two, four, and eight high-electron-mobility transistors (HEMTs) in the first, second, and third stages, respectively. The unit gate width of all HEMTs is 60 $\mu$m, with eight gate fingers. As the amplifier is targeted toward system integration, low input and output reflection coefficients are crucial to avoid standing-wave phenomena. Thus, we implemented a balanced architecture, using Lange couplers at the input and output.

All stages are matched reactively: two parallel low-loss output matching networks combine the output power of four HEMTs, each, and transform the impedance level to 50 Ω. The two signals are then combined using a Lange coupler on the output. The matching network design was carried out by first synthesizing passive equivalent circuits of the large-signal input and tradeoff load impedances. Next, low-loss prototype networks were designed using basic microstrip Process Design Kit (PDK) elements. Due to the desired compact layout and rather thick substrates, extensive coupling effects occur, especially in the final interstage matching networks (ISMNs, as seen in the inset in Fig. 1). As a result, the translation of the prototype networks to a layout first yielded poor electromagnetic (EM) responses. To improve this, space-mapping techniques [10], [11] were used extensively for each of the networks, which resulted in significantly improved EM-simulated matching bandwidth.

As a basis for large-scale power combining, we integrated the HPA MMIC into a self-contained split-block module (cf. Fig. 2). To reduce losses in the interface to the combiner, we use a standard WR-28 waveguide flange for the input and output. To allow for a radial combiner and splitter in the system center, the RF flanges are located on the same face of

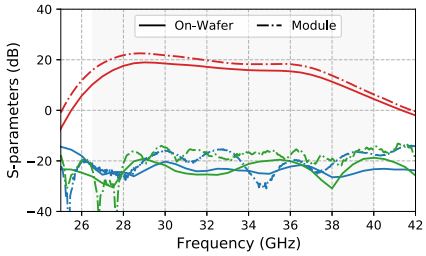


Fig. 3. Comparison of the developed HPA's small-signal measurements, both on-wafer and at the module's waveguide flanges.

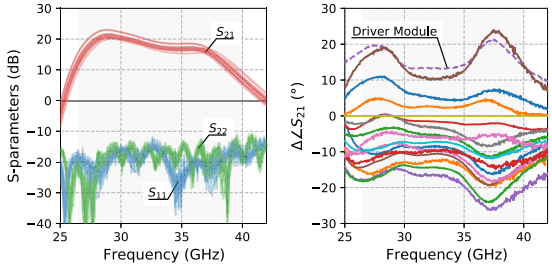


Fig. 4. Small-signal measurements of 17 modules. In (a), *S*-parameter magnitudes are shown, while (b) depicts the relative insertion phase offset.

the module. The waveguides are connected to the MMIC via *E*-field probes and short bond wires. The *E*-field probes were manufactured separately on a custom fused-silica substrate with a thickness of 135 $\mu$m. Furthermore, the module contains low-frequency stabilization elements and bias circuitry that merge the various bias voltages to a single gate and drain bus, which is routed to the bias connector.

The MMIC's small-signal measurement results are depicted in Fig. 3, both in the case of the on-wafer measurement and for the split-block module. Both measurements were acquired at a drain voltage of 15 V and a current density of 150 mA/mm. The module measurement shows a peak $S_{21}$ of 22.6 dB, while the on-wafer measurement exhibits a maximum of 19 dB. This difference can be attributed to the better thermal attachment in the module when compared to the on-wafer environment. As a result of the balanced architecture, the on-wafer input and output reflection coefficients are below −19.1 dB in the entire *Ka*-band. With values below −14.1 dB, the module exhibits slightly higher but still tolerable reflections, which are caused by the *E*-field probes and the bond wire transitions.

## IV. SSPA Development and Characterization

A total of 17 PA modules have been manufactured and individually characterized for use in the SSPA. Fig. 4(a) depicts the *S*-parameters between 25 and 42 GHz for all of them. Their $S_{21}$ exhibits a spread of below ±1.5 dB. Moreover, the relative small-signal phase difference $\Delta\angle S_{21}$ as shown in Fig. 4 indicates a phase spread of below ±25°. We also conducted individual module-level large-signal measurements at 30 GHz, which indicated a $P_{\text{out}}$ between 38.9 and 39.4 dBm and a *PAE* of 27.1± 1.5% at a constant $P_{\text{in}}$ of 21 dBm.

A simplified overview of the SSPA architecture is illustrated in Fig. 5 (top). It includes a waveguide splitter that divides the input signal into 16 individual parts of equal amplitude

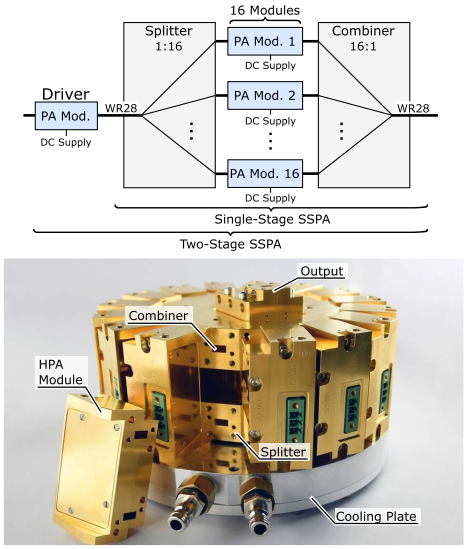


Fig. 5. Single- and two-stage SSPA system diagram (top) and photograph of the single-stage SSPA configuration including cooling plate (bottom). The system diameter is 16.4 cm.

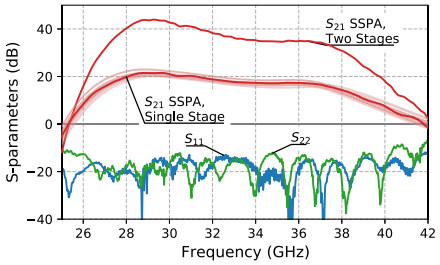


Fig. 6. Small-signal measurements of the one- and two-stage SSPA configurations and $S_{21}$ sweeps of all 17 modules (light red).

and phase. The 16 waveguide modules are fed by this signal—each contains one of the MMICs shown in Fig. 1. The modules are individually biased from a dedicated printed circuit board (PCB) (not shown). The amplified output signals are then combined using a radial combiner structure [12] identical to the splitter. Furthermore, in the two-stage setup, an additional PA module is connected to the splitter input, roughly doubling the SSPA's gain.

A photograph of the single-stage SSPA assembly can be seen in Fig. 5 (bottom). The SSPA's characterization was carried out after biasing each of the modules with $V_D = 15$ V and $i_D = 150$ mA/mm, which equals a quiescent supply current $I_D$ of 33.6 A. Fig. 6 depicts the small-signal measurement results. As can be seen, the single-stage $S_{21}$ is consistent with the single-module measurements (same plot, light red). Moreover, the SSPA's $S_{11}$ and $S_{22}$ exhibit very similar values to the characteristics of the single modules, which indicates good matching of the splitter/combiner system. In the two-stage setup, the transducer gain is roughly doubled, reaching a maximum of 44 and over 20 dB in the entire *Ka*-band.

The large-signal CW characterization was carried out using the measurement setup shown in Fig. 7 (top): three high-power loads are connected to the SSPA via a power splitter, the output power is detected using a 30-dB coupler. The results in 5 dB of gain compression are depicted at the bottom of Fig. 7. A maximum $P_{out}$ of 127 W at 31 GHz and

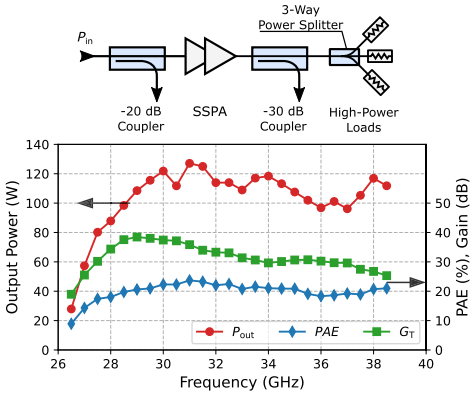


Fig. 7. Large-signal measurement setup and CW measurement results from the two-stage SSPA configuration in 5 dB of gain compression.

TABLE I
RECENT PUBLICATIONS OF WIDEBAND *Ka*-BAND SSPAS

| Ref. | # MMICs | Freq. GHz | $S_{21}$ dB | $P_{out}$ W | *PAE* % |
|---|---|---|---|---|---|
| [7] | 16 | 27–31 | 22–24 | 145–190 | 20–24 |
| [8] | 16 | 32–38 | 17–27 | 115–145 | 15–18 |
| [13] | 16 | 34–36 | 20–24 | 315–330* | 15–17 |
| [5] | 4 | 31–34 | 23–24 | 20–32 | 30–32 |
| [14] | 1+16 | 35–37 | n/a | 19–21 | 18–21 |
| [15] | 32 | 31–36 | n/a | 15–50 | 3–11 |
| [16] | 1+1+16 | 37–42 | 65 | 21–22 | 15–17 |
| **This** | 1+16 | 28–38 | 31–44 | 96–127 | 18–24 |

* Pulsed excitation, 50 % duty cycle.

power exceeding 100 W in a large part of the *Ka*-band were measured. Additionally, a *PAE* of close to 20% was measured in the same frequency range, showing close agreement with the single-module efficiency measurements. Comparison to recent publications of *Ka*-band SSPAs as depicted in Table I illustrates this work's favorable characteristics in bandwidth, efficiency, and also gain values.

## V. CONCLUSION

In this letter, we describe the design and characterization of a wideband SSPA system in the *Ka*-band frequency range. By using an advanced 100-nm GaN-on-SiC process and extensive EM simulations, we design a wideband PA which is subsequently integrated into a waveguide split-block module. In conjunction with waveguide-based power splitters and combiners, the modules form a two-stage 16-way SSPA. The SSPA characterization demonstrates a peak $P_{out}$ of 127 W and a peak gain of 44 dB. The unique wideband design enables a $P_{out}$ of more than 100 W in most of the *Ka*-band. To our knowledge, this is the most broadband high-power SSPA demonstrated in this frequency range to date.

## ACKNOWLEDGMENT

The authors would like to thank our colleagues in technology and technical services departments at the Fraunhofer Institute for Applied Solid State Physics (IAF) for their excellent contributions.

## REFERENCES


[1] C. F. Campbell, S. Nayak, M.-Y. Kao, and S. Chen, "Design and performance of 16–40 GHz GaN distributed power amplifier MMICs utilizing an advanced 0.15 $\mu$m GaN process," in *IEEE MTT-S Int. Microw. Symp. Dig.* , May 2016, pp. 1–4.

[2] V. D. Giacomo-Brunel *et al.*, "Industrial 0.15-$\mu$m AlGaN/GaN on SiC technology for applications up to Ka band," in *Eur. Microw. Integr. Circuits Conf.*, Sep. 2018, pp. 1–4.

[3] C. Ramella, C. Florian, E. Cipriani, M. Pirola, F. Giannini, and P. Colantonio, "Ka-band 4 W GaN/Si MMIC power amplifier for CW radar applications," in *Proc. Eur. Microw. Integr. Circuits Conf.*, Jan. 2021, pp. 33–36.

[4] R. Leblanc *et al.*, "6 W ka band power amplifier and 1.2 dB NF X-band amplifier using a 100 nm GaN/Si process," in *Proc. IEEE Compound Semiconductor Integr. Circuit Symp. (CSICS)*, Oct. 2016, pp. 6–9.

[5] N. Estella, E. Camargo, J. Schellenberg, and L. Bui, "High-efficiency, Ka-band GaN power amplifiers," in *IEEE MTT-S Int. Microw. Symp. Dig.*, Jun. 2019, pp. 568–571.

[6] J. Schellenberg *et al.*, "37 W, 75–100 GHz GaN power amplifier," in *IEEE MTT-S Int. Microw. Symp. Dig.*, May 2016, pp. 81–84.

[7] S. D. Yoon *et al.*, "Highly linear efficient power spatium combiner amplifier with GaN HPA MMIC at millimeter wavelength frequency," in *IEEE MTT-S Int. Microw. Symp. Dig.*, Aug. 2020, pp. 416–419.

[8] (Jan. 2020). Qorvo. *32–38 GHz Ka-Band GaN Amplifier*. [Online]. Available: https://www.qorvo.com/products/d/da007295

[9] D. Schwantuschke, P. Brückner, S. Wagner, M. Dammann, M. Mikulla, and R. Quay, "Enhanced GaN HEMT technology for E-band power amplifier MMICs with 1 W output power," in *Proc. IEEE Asia–Pacific Microw. Conf. (APMC)*, Nov. 2017, pp. 395–398.

[10] P. Neininger, L. John, P. Bruckner, C. Friesicke, R. Quay, and T. Zwick, "Design, analysis and evaluation of a broadband high-power amplifier for Ka-band frequencies," in *IEEE MTT-S Int. Microw. Symp. Dig.*, Jun. 2019, pp. 564–567.

[11] P. Neininger *et al.*, "Limitations and implementation strategies of interstage matching in a 6-W, 28–38-GHz GaN power amplifier MMIC," *IEEE Trans. Microw. Theory Techn.*, vol. 69, no. 5, pp. 28–38, Mar. 2021.

[12] P. Neininger *et al.*, "16-way Ka-band power combiner using novel waveguide transitions," *IEEE Trans. Microw. Theory Techn.*, 2022.

[13] (2021). Qorvo. *34–36 GHz 250 Watt GaN SSPA*. [Online]. Available: https://www.qorvo.com/products/d/da008125

[14] J.-P. Fraysse *et al.*, "A 20 W Ka-band radial solid-state power amplifier with 20% associated power-added efficiency," in *Proc. Eur. Microw. Integr. Circuits Conf.*, Oct. 2013, pp. 688–691.

[15] L. W. Epp, D. J. Hoppe, A. R. Khan, and S. L. Stride, "A high-power Ka-band (31–36 GHz) solid-state amplifier based on low-loss corporate waveguide combining," *IEEE Trans. Microw. Theory Techn.*, vol. 56, no. 8, pp. 1899–1908, Aug. 2008.

[16] R. Giofre, F. Costanzo, A. Massari, A. Suriani, F. Vitulli, and E. Limiti, "A 20 W GaN-on-Si solid state power amplifier for Q-band space communication systems," in *IEEE MTT-S Int. Microw. Symp. Dig.*, Aug. 2020, pp. 413–415.